
Article:
Wong-Stringer, M., Game, O.S., Smith, J.A. et al. (10 more authors) (2018) High-Performance Multilayer Encapsulation for Perovskite Photovoltaics. Advanced Energy Materials, 8 (24). 1801234. ISSN 1614-6832

https://doi.org/10.1002/aenm.201801234

High performance Multi-Layer Encapsulation for Perovskite Photovoltaics

Michael Wong-Stringer[1], Onkar S. Game[1], Joel A. Smith[1], Thomas J. Routledge[1], Bakhet A. Alqurashy[2], Benjamin G. Freestone[1], Andrew J. Parnell[1], Naoum Vaenas[1], Vikas Kumar[3], Majed O. A. Alawad[4], Ahmed Iraqi[4], Cornelia Rodenburg[3] and David G. Lidzey[1]*

[1]Department of Physics & Astronomy, University of Sheffield, Hicks Building, Hounsfield Road, Sheffield, S3 7RH, UK

[2]Department of Basic Science and Technology, Community Faculty, Taibah University, 30002 Al-Madina Al-Mounawara, Saudi Arabia

[3]Department of Materials Science and Engineering, University of Sheffield, Mappin St, Sheffield, S1 3JD, UK

[4]Department of Chemistry, University of Sheffield, Brook Hill, Sheffield, S3 7HF, UK

*Corresponding author, email d.g.lidzey@sheffield.ac.uk

Keywords: PVP, epoxy, perovskite solar cells, stability, lifetime, T80, encapsulation, solvent anneal

Supplementary Information

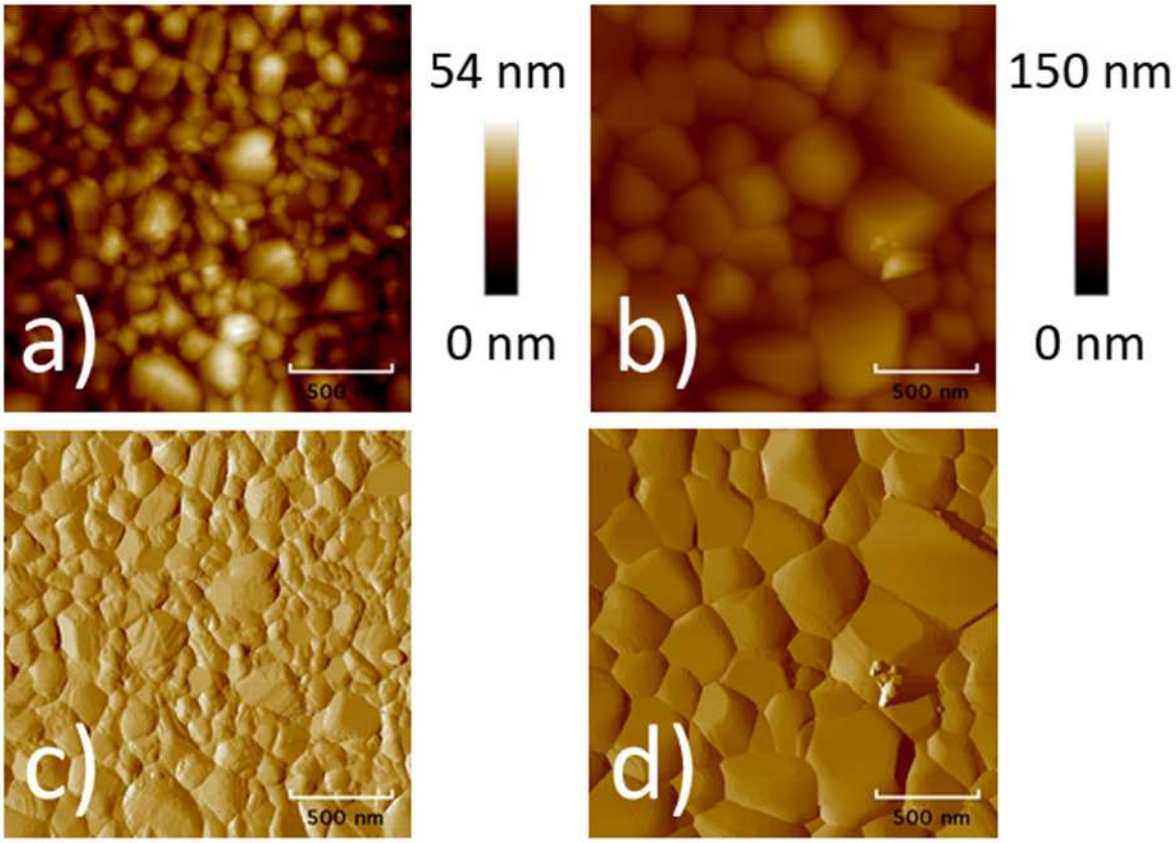

Figure S1: Atomic force microscopy height images of (a) MAPbI3 following thermal annealing and (b) MAPbI3 following an additional solvent anneal. The film Ra roughness average is 6.5 nm and 19 nm respectively. Films were deposited on ITO/poly-TPD. For completeness, the corresponding phase maps for (a) and (b) are shown in (c) and (d) respectively.

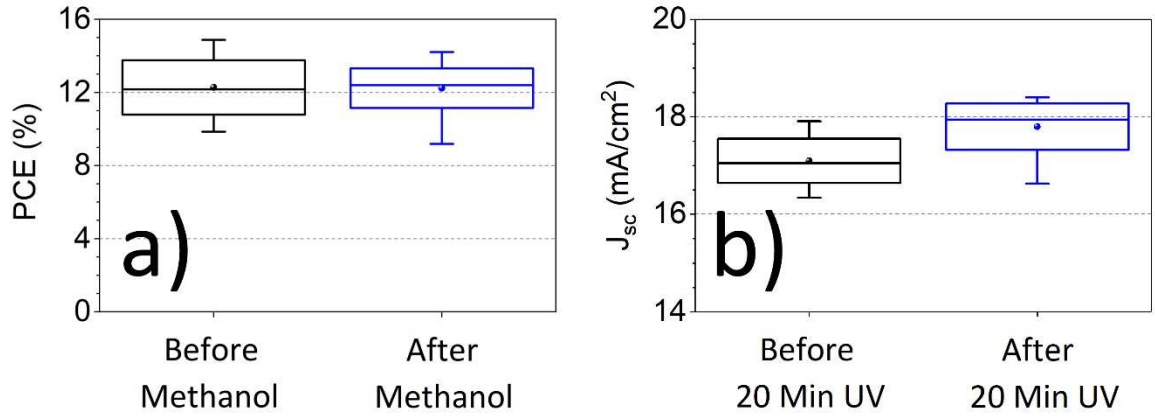

Figure S2: (a) PCE boxplots of PSCs with no solvent anneal and no encapsulation before (black) and after (blue) dynamically spin coating methanol at 6000 rpm on the completed PSCs. This confirms that the methanol used to deposit the PVP encapsulation does not alter the device performance. Data was obtained from N = 50 device measurements across 3 substrates (8 devices per substrate, metrics from reverse and forward sweeps included). (b) J_{sc} boxplots before (black) and after (blue) exposure to 20 minutes of UV light in N_2-GB. Here, devices were not encapsulated nor were they solvent annealed. This demonstrates that the UV light used to cure the epoxy does induce a statistically significant increase in J_{SC}.

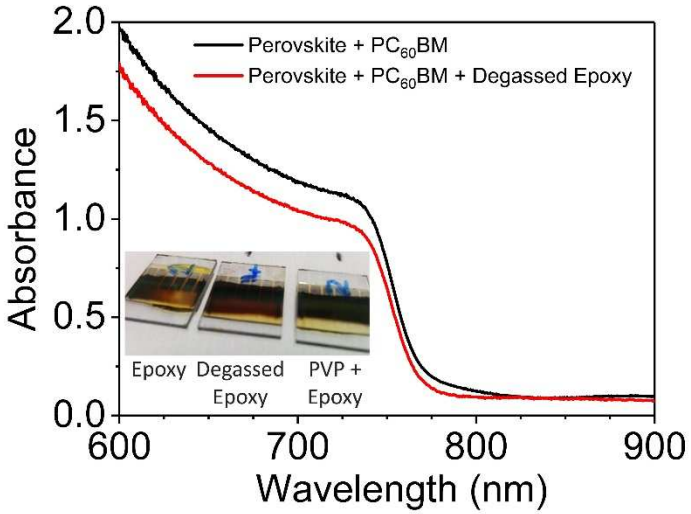

Figure S3: Absorbance of thin films on quartz coated glass of a thick $MAPbI_3$ /$PC_{60}BM$ stack before (black) and after (red) encapsulation with epoxy. Here, the epoxy has been 'degassed' under vacuum for 48 hours. This process is found to reduce (but not completely suppress) the effect of the encapsulation process that degrades the perovskite. The inset photograph shows the same effect for completed devices. Here, a device encapsulated with degassed epoxy appears darker (more absorbing) than a device encapsulated with untreated (non-degassed) epoxy. We find that the simple inclusion of a PVP interlayer prevents the damaging effect of the epoxy more than does the degassing procedure. Here, we have subtracted the absorbance of the encapsulation from that of the $MAPbI_3$ film.

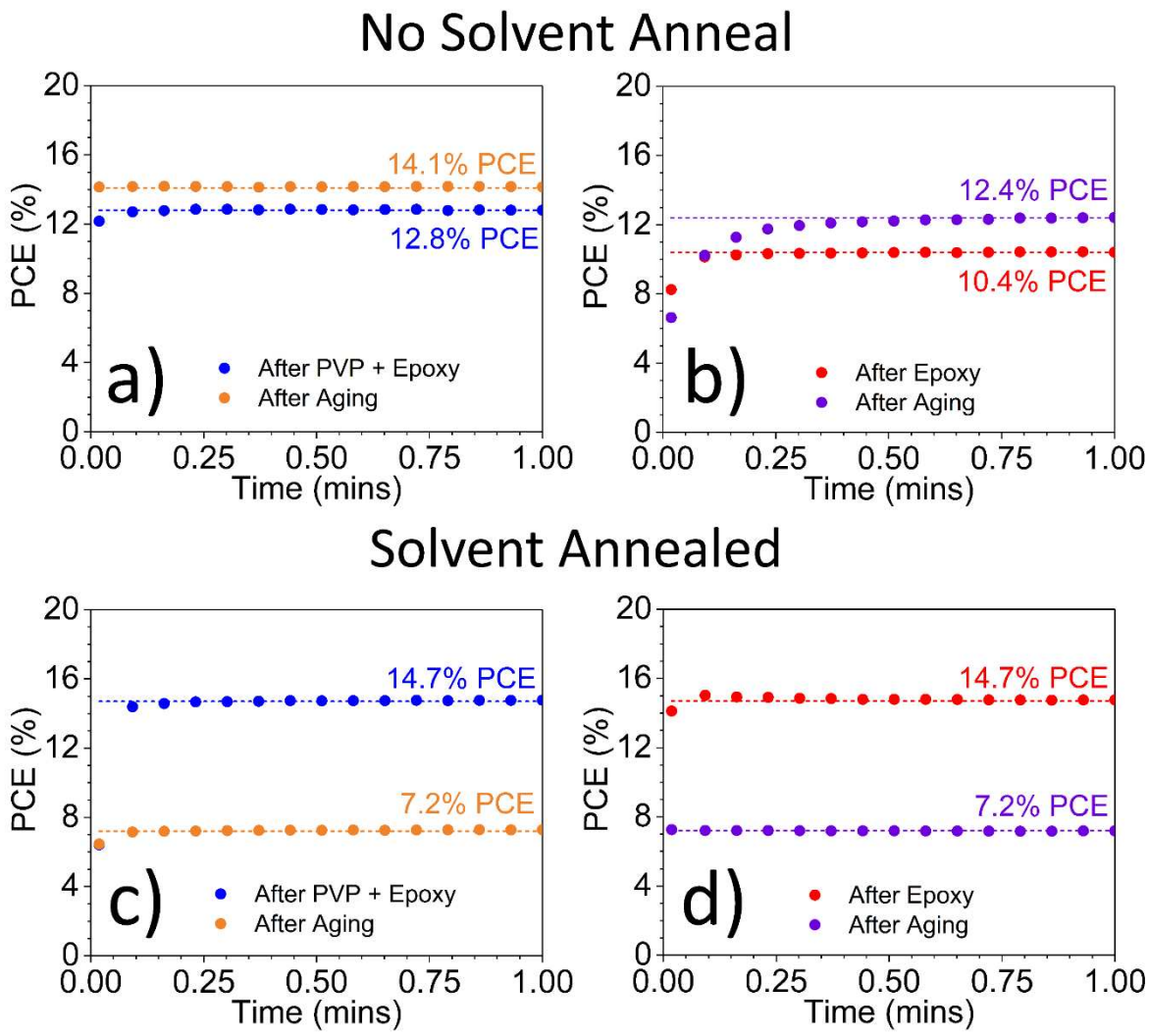

Figure S4: Stabilised PCE measurements of representative PSC sweeps shown in Figure 4c-f using the same plot colours as used in Figure 4. Part (a) shows stabilised PCEs of devices with no solvent anneal (non-SA) with devices encapsulated with PVP/epoxy, part (b) shows non-SA devices encapsulated with epoxy, part (c) shows solvent annealed (SA) devices encapsulated with PVP/epoxy and (d) SA encapsulated using just epoxy. Stabilised measurements were not recorded before encapsulation to minimise aging of the device.

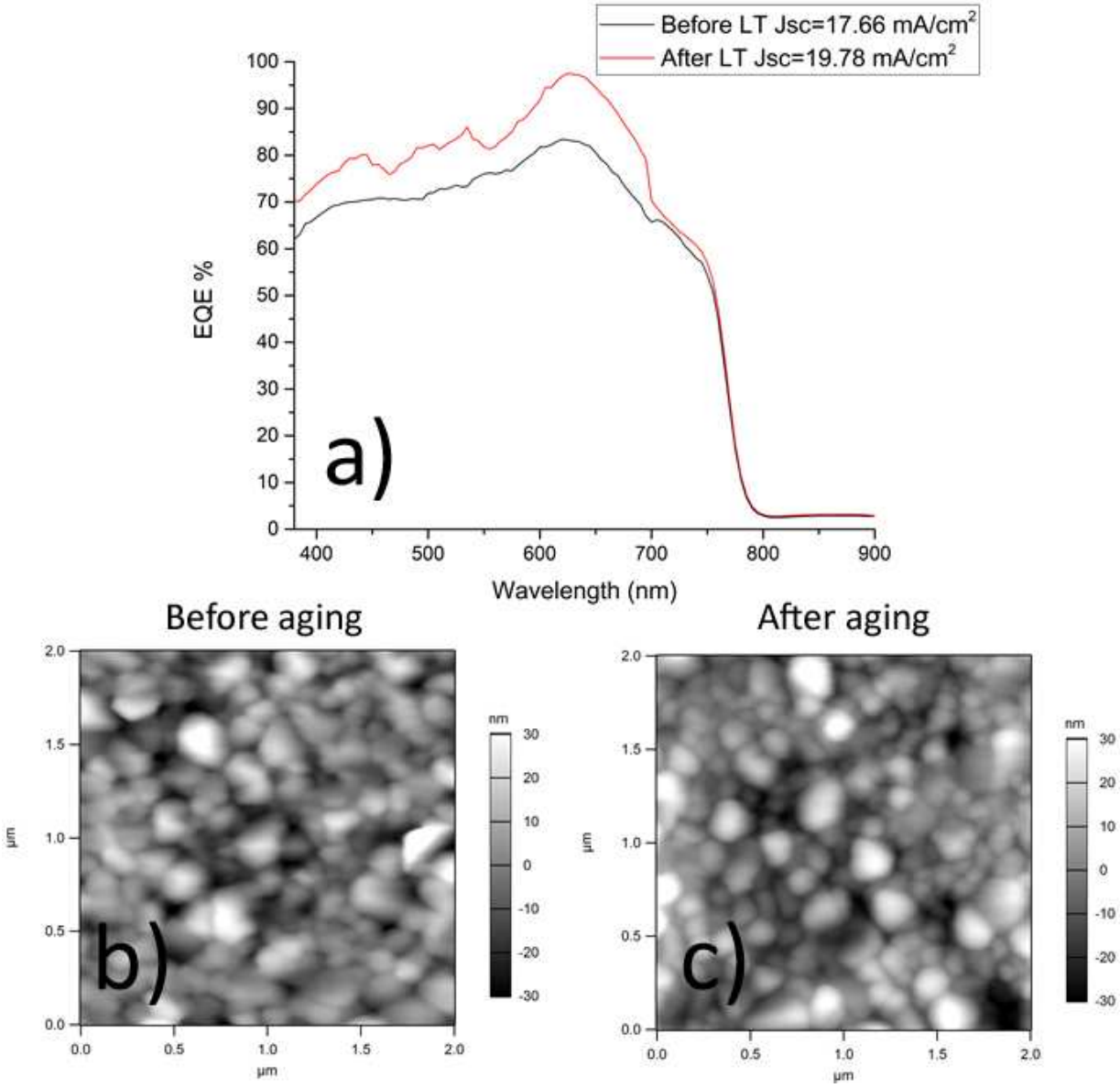

Figure S5: (a) EQE of a typical non-solvent annealed device (encapsulated with PVP and Epoxy) before (black) and after 18 hours of aging (red). No shift in the band edge is observed. (c) Atomic force microscopy height images before aging and (d) directly after aging, indicating that average grain size has not changed. Films were encapsulated with PMMA before overnight aging and then washed off before AFM measurement.

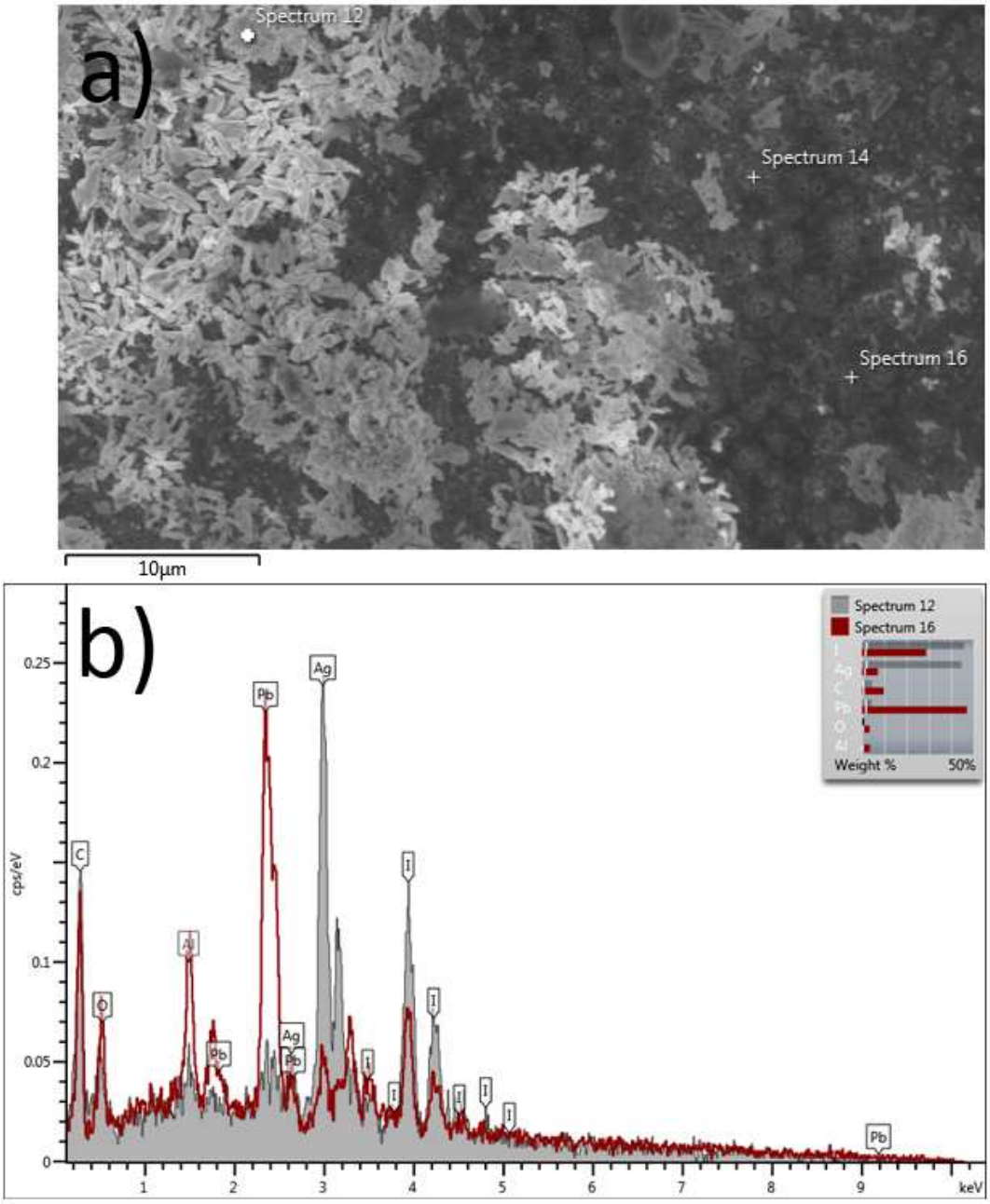

Figure S6: (a) Top view SEM showing locations of energy dispersive X-ray spectra presented in (b), showing an excess of silver and iodine in the dendrite features (spectrum 12) as compared to less degraded $MAPbI_3$ areas (spectrum 16).

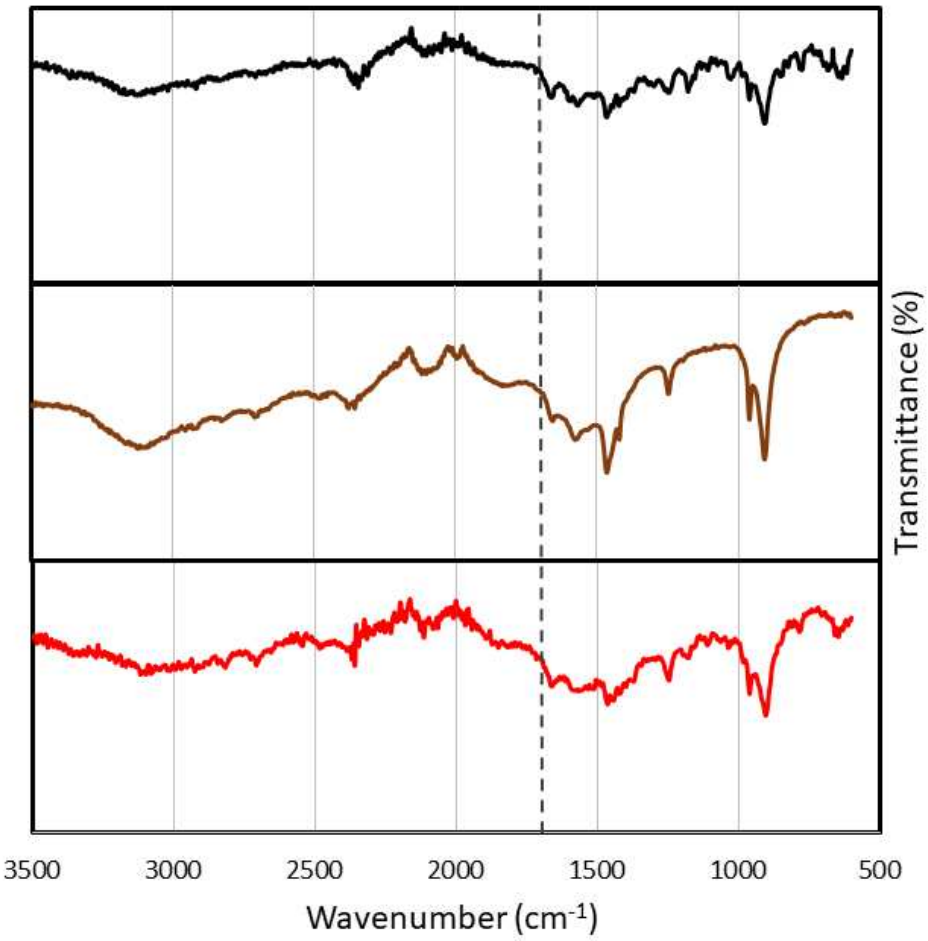

Figure S7: Fourier transform infrared (FTIR) spectra for a) MA:AC deposited $MAPbI_3$ (black), b) solvent annealed $MAPbI_3$ (brown) and c) "extreme" solvent annealed $MAPbI_3$ (high solvent volume and no subsequent annealing). We find that there is no observable carbonyl (C=O) stretch apparent around 1660-1690cm^{-1} (grey dashed line) as would be expected for dimethylformamide (DMF), indicating that there is very little residual solvent in the films following solvent annealing. All other frequencies are comparable to previous reports of $MAPbI_3$.[1] Full material preparation and analysis is described in methods.

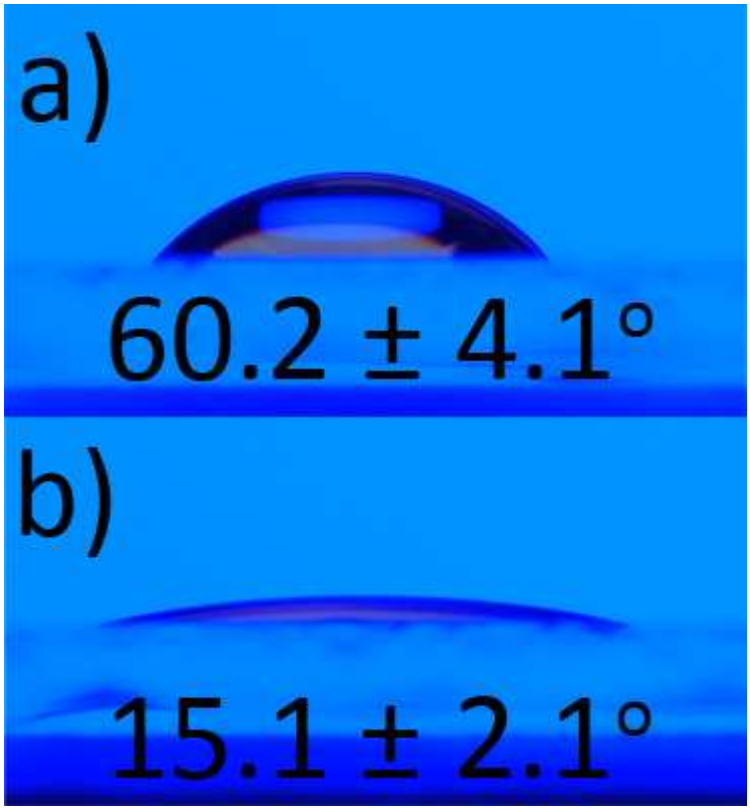

Figure S8: Contact angles of deionised water on both poly-TPD and PEDOT:PSS. The high contact angle of water upon poly-TPD demonstrates the hydrophobic nature of poly-TPD, while PEDOT:PSS is soluble in water and extremely hydrophilic. Because of the polar nature of solvents used with typical perovskites, the perovskite solution tends to dewet from a poly-TPD surface, however poly-TPD is largely moisture free and will thus improve PSC stability.

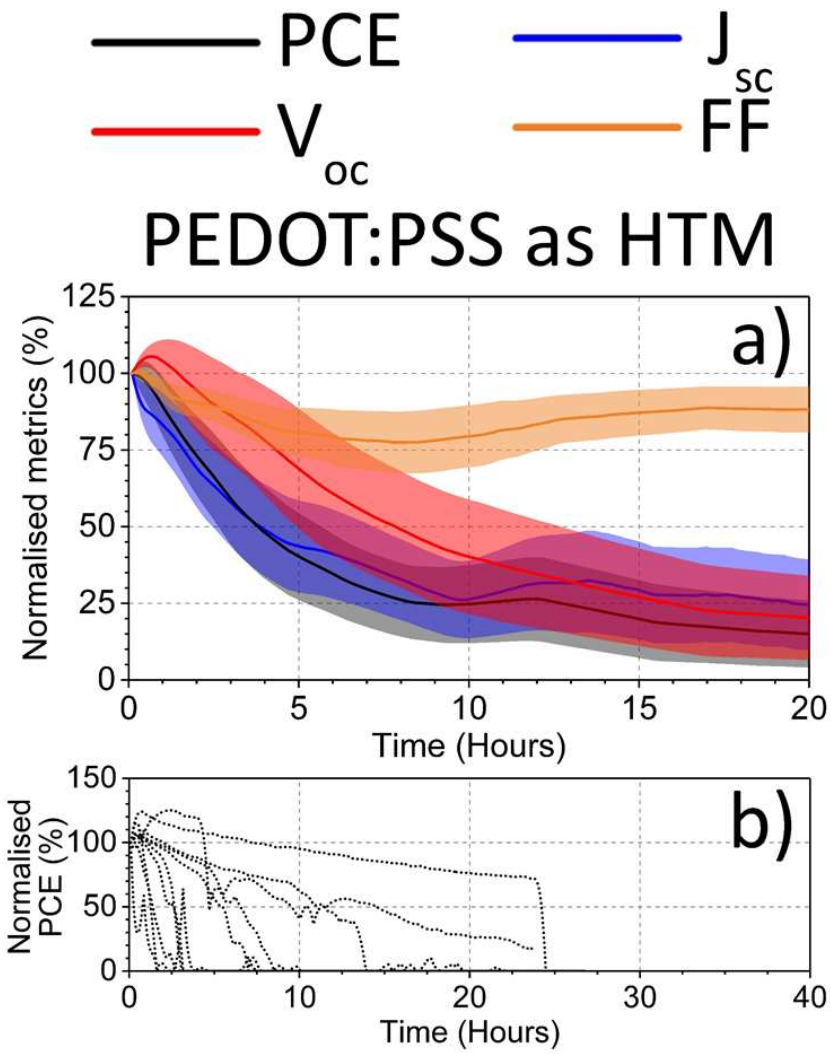

Figure S9: (a) Performance metrics (Black - PCE, J_{sc} - blue, V_{oc} - red, FF - orange) for PEDOT:PSS containing devices during device operation. This highlights the rapid decay of PSCs despite encapsulation with PVP and epoxy. We attribute the fast decay of these PCSs to moisture adsorbed onto the PEDOT:PSS surface that was sealed into the device during fabrication, and/or the acidic nature of PEDOT:PSS etching the ITO[2,3]. Solid lines represent the mean of each metric and the translucent band represents the standard deviation across all the devices. In part (b) dotted lines indicate the performance of individual devices over time.

Acknowledgements

This work was funded by the UK Engineering and Physical Sciences Research Council (EPSRC) via grants EP/M025020/1 'High resolution mapping of performance and degradation mechanisms in printable photovoltaic devices', EPSRC grant EP/N008065/1 'Secondary Electron Emission - Microscopy for Organics With Reliable Engineering-Properties', and EP/M014797/1 'Improved Understanding, Development and Optimization of Perovskite-based Solar Cells'. We also thank the EPSRC for PhD studentships via the University of Sheffield DTG account (T.R.) and from the Centre for Doctoral Training in New and Sustainable PV, EP/L01551X/1 (M.S., C.G., B.F., J.S.). We also would like to thank Dr James Kingsley, Dr Nick Scarratt, Claire Greenland, Emma Spooner, and Rachel Kilbride for useful discussions.

[1] X. Guo, C. McCleese, C. Kolodziej, A. C. S. Samia, Y. Zhao, C. Burda, *Dalt. Trans.* **2016**, *45*, 3806.

[2] W. Lee, M. Song, S. Park, S. Nam, J. Seo, H. Kim, Y. Kim, *Sci. Rep.* **2016**, *6*, 1.

[3] C. Bracher, B. G. Freestone, D. K. Mohamad, J. A. Smith, D. G. Lidzey, *Energy Sci. Eng.* **2017**, 6. 35.